

Adelinda A. Yee
Randal Babiuk
Joe D. J. O'Neil*
Department of Chemistry
University of Manitoba
Winnipeg, Manitoba R3T 2N2,
Canada

The Conformation of an Alamethicin in Methanol by Multinuclear NMR Spectroscopy and Distance Geometry / Simulated Annealing

The solution conformation of the antibiotic peptide alamethicin was investigated using multinuclear spectroscopy and the distance geometry/simulated annealing algorithms from the program DSPACE. ^1H -, ^{13}C -, and ^{15}N -nmr chemical shifts and homonuclear ^1H coupling constants suggest that the molecule is flexible in the vicinity of Gly-11 and Leu-12. The temperature dependence of the amide proton chemical shifts indicates that there is flexibility in the middle of the 20 residue peptide and provides evidence that, at the very N-terminus, the molecule adopts a 3_{10} -helical conformation. The large differences in the ^{13}C chemical shifts of the pro-R and pro-S methyls of the α -aminoisobutyric acid residues were used to constrain those residues to the right-handed helical conformation in the distance geometry/simulated annealing algorithms. A family of 24 structures was generated but did not converge to a common conformation when superimposed over the entire polypeptide sequence. The molecules did converge to a helical conformation over residues 1–10 and residues 13–18. The lack of convergence when the entire lengths of the molecules are superimposed is explained by the flexibility of the peptide near Gly-11/Leu-12. The results suggest that the protein consists of two helices connected by a flexible "hinge." The flexibility of the molecule is discussed with respect to the macrodipole model of voltage gating. © 1995 John Wiley & Sons, Inc.

INTRODUCTION

The amino acid α -aminoisobutyric acid (Aib) is an analogue of alanine that consists of an α -methyl group in place of the usual αH . Steric interactions involving the α -methyls are thought to restrict the conformational space accessible to Aib to the right- and left-handed α - and 3_{10} -helices. Empirical energy calculations on Aib, and on D- and L-Ala, suggest that about 30 kJ/mole is required to interconvert the right- and left-handed conformers of Aib.^{1–3} The high helical propensity of Aib has been confirmed by the crystal structures of more than 60

Aib-containing peptides^{4–7} and in solution by the helical structure of an eight residue peptide.^{8,9} These observations have led to the incorporation of Aib in the helical segments of synthetic peptides and proteins.¹⁰

The Aib residue is found naturally occurring in alamethicin, a 20 residue, hydrophobic, antibiotic peptide produced by the fungus *Trichoderma viride*¹¹ as well as in several other similar molecules.⁴ The structure of alamethicin crystallized from an acetonitrile:methanol solution (10:1) was determined by x-ray diffraction.¹² Three molecules are observed in the asymmetric unit, and their con-

Received August 16, 1994; accepted April 18, 1995.

* To whom correspondence should be addressed.

Biopolymers, Vol. 36, 781–792 (1995)

© 1995 John Wiley & Sons, Inc.

CCC 0006-3525/95/060781-12

formations are all α -helical in the N-terminal half of the peptide, and α - or 3_{10} -helical in the C-terminal half. Alamethicin has also been studied in several organic solvents, and in aqueous solutions containing detergent and lipid by nmr, CD, and ir spectroscopies (for reviews, see Refs. 13 and 14). A range of conformations has been observed from mostly disordered in water to mostly helical in some organic solvents. Recently, an α to 3_{10} transition was observed in solution by nmr spectroscopy upon sequence permutation of small Aib-containing peptides.¹⁵ This conformational transition has also been studied using molecular mechanics calculations on homopolymers of Aib of various lengths.¹⁶ Knowledge about the conformation and dynamics of alamethicin in solution is essential for a full appreciation of the influences of Aib residues on peptide structure and dynamics and of their usefulness in protein design. It could also lead to a better understanding of the mechanism by which peptides such as alamethicin form voltage-gated ion channels in lipid bilayers.¹⁴ In the following, we report the solution conformation of alamethicin based on nmr-restrained distance geometry calculations, ^1H -, ^{13}C -, and ^{15}N -nmr chemical shifts, and the temperature dependence of the amide proton chemical shifts.

MATERIALS AND METHODS

NMR Spectroscopy

Trichoderma viride produces a mixture Aib-containing peptides with different sequences. An unlabeled alamethicin peptide was purified by high performance liquid chromatography as described previously,¹⁷ dissolved in 0.55 mL CD_3OH to a concentration of approximately 3 mM, and placed in a 5 mm nmr tube (Wilmad 535). The apparent pH was 8.4. The nmr experiments at 500 MHz were done on a Bruker AMX 500 nmr spectrometer using a 5 mm inverse broadband probehead. A two-dimensional $^1\text{H}/^{13}\text{C}$ heteronuclear single quantum correlated spectroscopy (HSQC) spectrum¹⁸ was acquired at 300 K with decoupling of ^{13}C during the 0.39 s acquisition period using the GARP sequence.¹⁹ The experiment was phase sensitive using time-proportional phase incrementation for quadrature detection.²⁰ The ^1H sweep width was 5263 Hz and the ^{13}C sweep width was 22,700 Hz. A total of 512 t_1 spectra were collected, each consisting of 4K data points. The data were zero filled to 1K in F_1 only. A $\pi/2$ -shifted \sin^2 filter was applied to ω_1 and ω_2 before Fourier transformation; the spectra were baseline corrected by subtracting a 5th order polynomial from both dimensions. The internal ^1H reference was disodium 2,2-dimethyl-2-silapentane-5-sulfonate (DSS)

and the ^{13}C reference was $^{13}\text{CD}_3\text{OH}$, which was set to 49.3 ppm. Some new nuclear Overhauser effect (NOE) cross peaks were detected, and some previous ambiguities resolved, in a two-dimensional rotating frame NOE spectroscopy (ROESY) spectrum of a 50:50 mixture of ^{15}N -labeled and unlabeled peptide acquired as previously described.¹⁷

The temperature-dependence of the NH chemical shifts in CD_3OH were determined by acquiring one-dimensional ^1H spectra of approximately 3 mM ^{15}N -labeled peptide from 230 to 340 K. The water resonance was preirradiated for 1 s, the observe pulse was 15 μs , and 128 scans were acquired. The ^1H sweep width was 5952 Hz and the acquisition time was 1.5 s. The amide proton chemical shifts were plotted against temperature and a least-squares fit to the equation of a straight line used to extract the slopes.

Calculations of Chemical Shift Differences ($\Delta\delta$)

Most of the protons in the ^1H -nmr spectra of alamethicin were assigned previously.^{17,21} Assignment of the ^{13}C resonances of alamethicin was done using the previously assigned ^1H resonances and a $^1\text{H}/^{13}\text{C}$ heteronuclear correlation map (Figure 1). The resonance assignments agree with those published²² except that the βC and γC assignments have been reversed for both Gln-18 and Gln-19. Some of the Aib C^βH_3 methyl protons were assigned during the structure determination as described below.

Except for the $^{13}\text{C}\beta$ resonances, average ^1H , ^{13}C , and ^{15}N random coil chemical shifts for non-Aib amino acids were taken from the values compiled.²³ The average $^{13}\text{C}\beta$ random coil values were taken from values calculated.²⁴ Chemical shift differences between the average random coil chemical shifts and the chemical shifts (δ) for alamethicin were calculated as $\Delta\delta = \delta^{\text{obs}} - \delta^{\text{rc}}$ (δ^{obs} : measured chemical shift in alamethicin; δ^{rc} : random coil chemical shift). There are no random coil chemical shift data available for Aib residues. The differences between the chemical shifts of Aib-1 and those of the other Aibs were calculated as $\Delta\delta^{\text{Aib}-n} = \delta^{\text{Aib}-n} - \delta^{\text{Aib}-1}$.

Distance Restraints

ROESY spectra were acquired with 300 and 600 ms mixing times¹⁷ and the volumes of the cross peaks integrated using the UXNMR software from Bruker. Interproton distances were calculated from the volumes of the 300 ms ROESY using the isolated spin pair approximation and setting the average methylene cross-peak volume to 1.8 Å. This gave reasonable distances for $d_{\alpha\beta}(i,i)$, $d_{\alpha\text{N}}(i,i)$, $d_{\alpha\text{N}}(i,i)$, and $d_{\alpha\text{N}}(i,i+1)$. For example, the strongest $d_{\alpha\beta}(i,i)$ cross peak (Q18) yielded a distance of 2.2 Å and the expected range of distances is from 2.1 to 2.9 Å.²⁵ The calculated interproton distances were separated into 4 groups accordingly: < 3.0, 3.0–3.5, 3.5–4.0, and 4.0–4.5 Å. Upper distance restraints for distance geometry

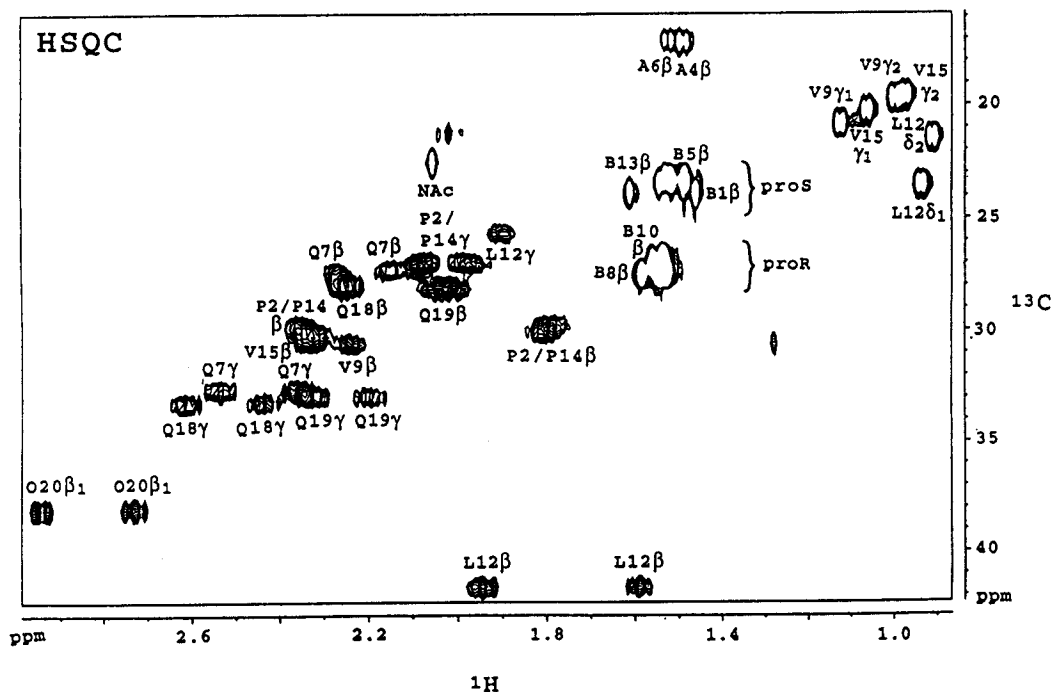


FIGURE 1 Aliphatic region of a ^{13}C - ^1H HSQC spectrum of unlabelled alamethicin in CD_3OH acquired at 500 MHz. The Aib *pro-R* and *pro-S* ^{13}C - ^1H methyl cross peaks were assigned assuming a right-handed helical conformation. The internal ^1H reference was DSS and the internal ^{13}C reference was the $^{13}\text{CD}_3\text{OH}$ signal, which was set to 49.3 ppm. The number of scans was 128 for each of 512 t_1 increments.

and simulated annealing calculations were the upper limits of the 4 groups of interproton distances. For NOEs involving methyl resonances, an additional 0.5 Å was added to the upper distance restraint.^{26,27} No NOE-derived lower distance restraints were used. Initial structures were observed to have distorted bond angles and distances defining the two proline rings. This was alleviated by raising the distance restraints for the proline hydrogens separated by 3 and 4 bonds to 3.5 and 4.0 Å, respectively. Spin-coupling interactions $^3J_{\alpha\text{N}}$ (three bond scalar coupling constant between the alpha and amide hydrogens) were measured previously on uniformly ^{15}N -labeled alamethicin in which the substitution of ^{15}N for ^{14}N significantly narrows the attached ^1H resonances permitting accurate coupling constant determination from one-dimensional spectra.¹⁷ For amino acids 4, 6, 7, 9, and 18, upper and lower distance restraints for $d_{\alpha\text{N}}$ (i, i) were set to 2.6 and 2.8 Å, respectively, based on measured $^3J_{\alpha\text{N}}$ less than 6 Hz for these residues.²⁵ These restraints are qualitatively confirmed by the ^{13}C chemical shifts of the αC resonances (see Results). In total, 167 distance restraints were determined. Of these, 77 were intraresidue restraints, 5 of which were calculated from $^3J_{\alpha\text{N}}$ coupling constants, and 16 constraints were imposed to restrain the Aib residues to the right-handed helical conformation (see below). The rest of the restraints comprised 50 sequential and 19 medium-range ($[i - j] = 2-4$) interproton distances. Three families of struc-

tures were generated: one in which the Aib residues were unconstrained, one in which the Aib residues were constrained to the right-handed helical conformation, and one in which 11 amide protons with slopes greater than -2.5 ppb/degree (see Figure 3A) were constrained to be hydrogen bonded. The lower and upper N to O distances were set to 2.65 and 3.2 Å, respectively, and the H_N to O distances to 1.65 and 2.2 Å, respectively.²⁸ Constraining the Aib residues to be helical resulted in a family of structures that refined more rapidly to structures with significantly lower penalties than could be achieved in the absence of the constraint.

Prochiral centers were dealt with as follows²⁸: The *pro-R* and *pro-S* C^βH protons were allowed to float between the two positions, the final positions in the structures being determined by the NOEs to the protons. Initially, the *pro-R* and *pro-S* C^βH_3 methyls of the Aibs were dealt with similarly. This resulted in molecules with Aib residues in the left-handed helical conformation, unlikely considering the abundance of L-amino acids. On the basis of the ^{13}C chemical shifts of the *pro-R* and *pro-S* C^βH_3 methyl resonances (see Results), all Aib residues were restricted to the right-handed helical conformation by constraining the distance between the NH proton and *pro-R* methyl carbon to between 2.95 and 3.25 Å, and by restricting the carbonyl oxygen to *pro-R* methyl carbon distance to between 2.55 and 2.90 Å (see Results/Discussion). This necessitated shutting off the floating

chirality and making stereospecific assignments of the Aib methyls. This was done by assigning an *NOE* to one of the prochiral methyls, generating structures, and checking for penalty violations in the structures at the residue of interest. In general, when an assignment was incorrect the penalties of all the structures were high and the incorrect Aib was distorted. When the assignment was corrected the total penalties were smaller, including those of the Aib residues. In this fashion the *pro-S* methyl ^1H resonances of Aib residues 1, 8, 10, and 14, and the *pro-R* methyl of Aib-9, were stereoassigned.

Structure Calculations

Alamethicin structures were calculated using the program DSPACE 4.0 (Hare Research, Inc). The calculations were done semiautomatically using published²⁸ DSPACE macros. Initially, a distance matrix was created and triangle inequality smoothing done using the upper and lower experimental distance constraints described above. The default lower distance bounds are the sums of the van der Waals radii for nonbonded atoms except for atoms that can form hydrogen bonding partners, in which case the lower distance bounds are allowed to be smaller than the van der Waals radii. The first trial structure was generated by a random embed of the bounds matrix, and this structure was subsequently refined to a relatively high penalty of 2.4 \AA^2 . Forty-eight starting structures were generated by scattering the coordinates of the first refined structure by a vector of random orientation and magnitude less than 20 \AA . These structures were then refined with the DSPACE four-dimensional simulated annealing and conjugate gradient minimization routines. Initially, experimental distance constraints were weighted about ten times higher than the primary constraints (bonds, angles, and van der Waals interactions); the experimental constraints were gradually lowered and the primary constraints gradually elevated until the two converged at the end of the refinement. After two stages of refinement, 35 structures had penalties less than 0.35 \AA^2 and were put through a third round of refinement. The result was a family of structures consisting of 24 molecules with penalties less than 0.13 \AA^2 . Those structures with Aib residues in the left-hand helical conformation were further annealed until all Aibs were in the right-hand helix. This always resulted in molecules with lower or unchanged penalties. The final family of 24 molecules all had penalties less than 0.06 \AA^2 . The errors reported are the value of 1 standard deviation.

RESULTS

Chemical Shifts, Secondary Structure, and Dynamics

Figure 1 shows the aliphatic region of the $^1\text{H}/^{13}\text{C}$ HSQC spectrum obtained at 300 K and used to as-

sign the ^{13}C resonances of alamethicin. Assignment of the Aib *pro-R* and *pro-S* regions of the spectrum follows the suggestion of Jung et al.⁴—that in a right-handed helical conformation the *pro-R* methyl is proximate to the Aib carbonyl oxygen, causing it to be deshielded relative to the *pro-S* carbon. The residue-specific assignments, which have not been previously published, were facilitated by assignment of the Aib methyl protons in a $^{15}\text{N}/^1\text{H}$ two-dimensional heteronuclear multiple quantum correlated spectroscopy spectrum.¹⁷ For example, the upfield methyl protons of residues 1 and 5 are resolved well enough to permit assignment of their respective *pro-S* carbon resonances (see Figure 1). The same is true of the downfield methyl protons of residues 13, 8, and 10. Because of spectral overlap in Figure 1, no Aib residue has both its *pro-R* and *pro-S* methyl carbon assigned. However, a reasonable assumption is that each Aib residue contributes one resonance to each of the *pro-R* and *pro-S* regions.

Wishart et al.²³ have pointed out the usefulness of ^1H , ^{13}C , and ^{15}N chemical shifts as indicators of secondary structure and dynamics in proteins. One of the best indicators of secondary structure is the $^{13}\text{C}\alpha$ resonance.^{23,24} Figure 2A shows the chemical shift differences between the $^{13}\text{C}\alpha$ chemical shifts of the non-Aib amino acids in alamethicin and the average random coil $^{13}\text{C}\alpha$ chemical shifts compiled.²³ Carbon resonances shifted downfield of the random coil frequencies by more than 1 ppm are suggestive of a helical conformation, and in alamethicin those residues span Pro-2 to Val-9 and Pro-14 to Gln-18 (Figure 2A). (Residues 16 and 17 are Aibs.) Phenylalaninol-20 (Pho-20) is the only residue that exhibits an upfield $^{13}\text{C}\alpha$ shift characteristic of a β -sheet, or extended, conformation. The $^{13}\text{C}\alpha$ resonances of Gly-11, Leu-12, and Gln-19 occur near the random coil chemical shifts for those residues.

The chemical shifts of the rest of the assigned nuclei in alamethicin exhibit similar patterns. Figure 2B shows that the $\text{C}\alpha\text{H}$ chemical shifts of Gly-11, Leu-12, and Pro-14 are near their random coil values, whereas most of the rest of the residues are shifted upfield characteristic of the helical conformation. Figure 2C indicates that the NH resonances of Gly-11 and Leu-12 are close to the values expected for the random coil conformation. This figure also shows the shifts of the Aib NHs relative to the NH of Aib-1 (open bars) and suggests that Aib-1 and Aib-13 occur in regions of the peptide that are unstructured. Similar results were ob-

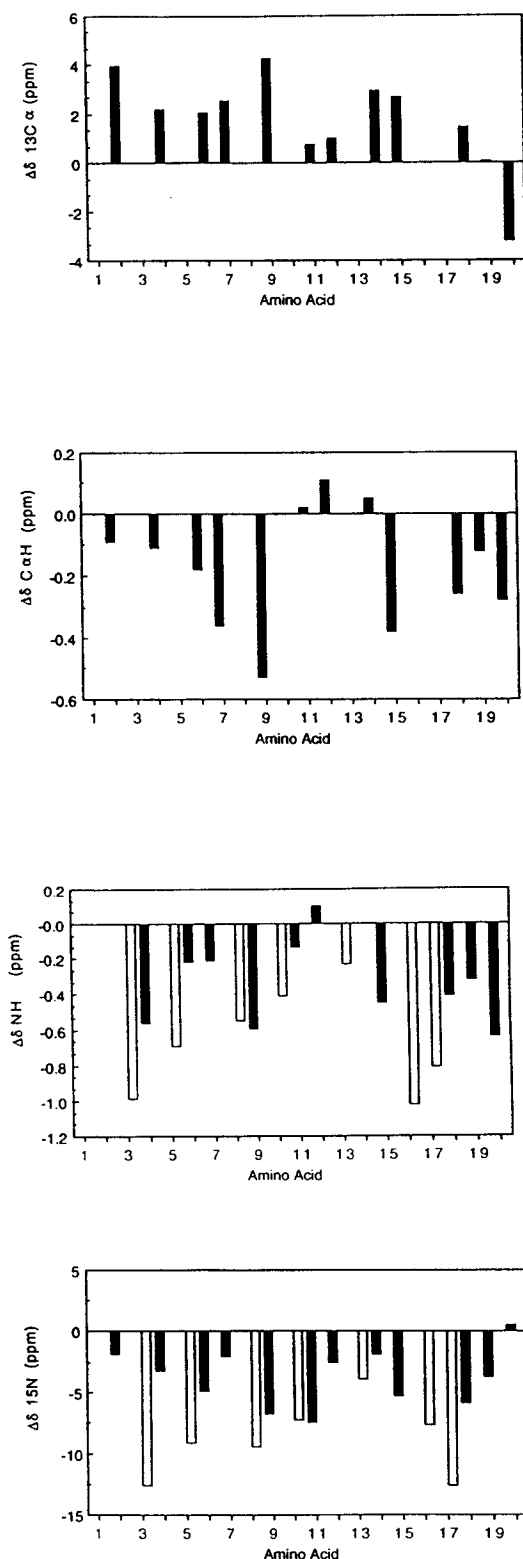


FIGURE 2 Differences ($\Delta\delta$) between observed chemical shifts (δ^{obs}) and random coil chemical shifts (δ^{rc}) are plotted for each amino acid in alamethicin for (A) $^{13}\text{C}\alpha$, (B) $\text{C}\alpha\text{H}$, (C) NH, and (D) ^{15}N . Open bars represent Aib residues and closed bars represent non-Aib residues.

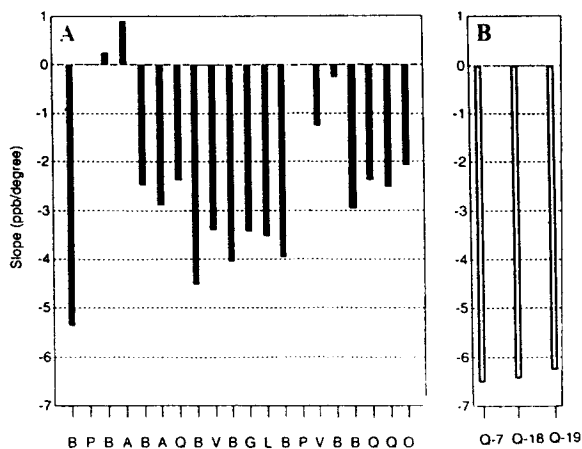


FIGURE 3 The temperature dependence of the side-chain (panel A; open bars) and backbone (panel B; closed bars) amide chemical shifts of alamethicin in methanol as a function of amino acid residue.

served for the ^{15}N (Figure 2D), $\text{C}\beta\text{H}$, and $^{13}\text{C}\beta$ shifts (data not shown).

Temperature Dependence of Amide Proton Chemical Shifts

The temperature dependence of the amide proton chemical shift is often used to detect intramolecular hydrogen bonding in proteins, and in the case of Aib-containing peptides has been used to distinguish between α and 3_{10} conformations.¹⁵ Figure 3 shows the slopes of the amide proton chemical shifts of alamethicin for the backbone (panel A; solid bars) and side-chain (panel B; open bars) amides. The largest slopes, (-5.3 to -6.4 ppb/degree) belong to the backbone amide of Aib-1 and the side-chain amides of the Gln residues and suggests that these are not intramolecularly hydrogen bonded. The backbone amides between Aib-8 and Aib-13 have slopes between -3 and -4.5 ppb/degree, possibly indicating weak intramolecular bonding in the middle of the molecule.¹⁵ Between Aib-5 and Gln-7 and between Aib-16 and Pho-20 the slopes are smaller yet, ranging from -3 to -2 ppb/degree. This is strongly indicative of a hydrogen-bonded state in these two regions.¹⁵ The smallest slopes belong to the two residues following each of the proline residues. The slopes of Aib-3 and Ala-4 are positive, and those of Val-15 and Aib-16 are greater than -1.2 ppb/degree. In a linear conformation the only carbonyl oxygen available to hydrogen bond with the NH of Aib-3 belongs to the N-terminal acetyl and would constitute

a 3_{10} interaction similar to those observed in small Aib-containing peptides.¹⁵ The small slope for the NH of Ala-4 suggests a second 3_{10} interaction between Aib-1 and Ala-4.

Distance Geometry Structures

Table I summarizes the structural statistics for the 24 alamethicin distance geometry (DG) structures generated with NOE, J -coupling, and Aib chemical shift constraints. The total penalties for the structures range from 0.034 to 0.054 Å² with a mean penalty of 0.042 ± 0.006 Å². The maximum individual violation is 0.066 Å.

The 24 DG structures superimpose with an average backbone (N, C α , C') rms deviation (rmsd) of 2.6 ± 0.8 Å, suggesting that the family has not converged to a common conformation. If we assume that the ends of the molecule are not well determined because of a lack of NOEs beyond the ends, and reduce the region of comparison to span

the molecules from Ala-4 to Aib-17, the average rmsd drops to 1.7 ± 0.4 Å, yet this is still too high to suggest convergence to a common structure. However, if the molecules are superimposed from Aib-1 to Aib-10, the average backbone rmsd drops to 1.0 ± 0.3 Å. Similarly, the 24 DG/simulated annealing (SA) structures superimpose from Leu-12 to Gln-17 with an average backbone rmsd of 0.54 ± 0.25 Å. Figure 4 shows the backbone conformation for 9 structures in the family superimposed over the region from Aib-1 to Aib-10, and Figure 5 shows 9 molecules superimposed over the region from Leu-12 to Aib-17. The family of 24 molecules superimpose on the 3 crystal structures¹² with an average backbone rmsd of 0.95 ± 0.30 Å over the region 1–10 and 0.52 ± 0.21 Å over the region from residues 12 to 17.

The DG/SA structures were also superimposed over a 6 residue segment that was moved one residue at a time along the peptide. The average backbone (N, C α , C') rmsd is plotted in the middle of the moving window in Figure 6. The variation in average rmsd suggests that there are two well-defined regions of structure, one centered at residue 8 and the other centered at residue 15. Significantly less well determined is the region centered on residue 12. The data also suggest that the ends of the molecule are less well determined than the interior segments. This is to be expected of an nmr structure as there can be no NOE contacts beyond the ends of the molecule. Disorder at the ends of the peptide is not observed to the same extent in a similar plot that compares the average backbone rmsds of the three crystal structures¹² over the same 6 residue moving window. However, the crystal structures also appear to show more variability in structure in the C-terminus than in the N-terminus.

The distribution of backbone Φ and Ψ angles in the family are illustrated in a Ramachandran plot shown in Figure 7A, and a plot of the average backbone dihedral angles and their confidence limits shown in Figure 7B. These plots indicate that the molecules are generally helical but that Gly-11, in the middle of the molecule, and Gln-18 and Gln-19, at the C-terminus, are the least constrained residues. Slightly better constrained are Ala-4 and Ala-6, in the N-terminus, and Leu-12 in the middle. The rest of the molecule is well determined.

Two other families of structures were also generated. In the first, no constraints were placed on the conformations of the Aib residues. In general, the structures (not shown) consist of two helices

Table I DG/SA Restraints and Structural Statistics

Distance Restraints		
Intraresidue	77	
$^3J_{\alpha N}$	5	
Aib $^{13}C\beta$	16	
Sequential	50	
Medium Range ($[i-j] = 2-4$)	19	
Total	167	
Mean restraints/residue	7.3	
Structural Statistics for the 24 DG Structures (Å ²) ^{a,b}		
Mean total penalty	0.042 ± 0.006 Å ²	
Max/min penalty	0.054/0.034 Å ²	
Max individual violation	0.066 Å	
Mean Pairwise RMSD (Å) ^b for N, C α , and C'		
	DG/SA Structures	DG/SA vs X-Ray Structures ^c
Residues 1–20	2.6 ± 0.8	2.6 ± 0.9
Residues 4–17	1.7 ± 0.4	1.6 ± 0.6
Residues 1–10	1.0 ± 0.3	0.95 ± 0.30
Residues 4–9	0.54 ± 0.21	0.55 ± 0.18
Residues 12–17	0.54 ± 0.25	0.52 ± 0.21

^a The penalty is the squared sum of the distance violations in Å².

^b The errors are 1 standard deviation.

^c The coordinates for the crystal molecules were obtained from the Brookhaven Protein Data Bank.⁷

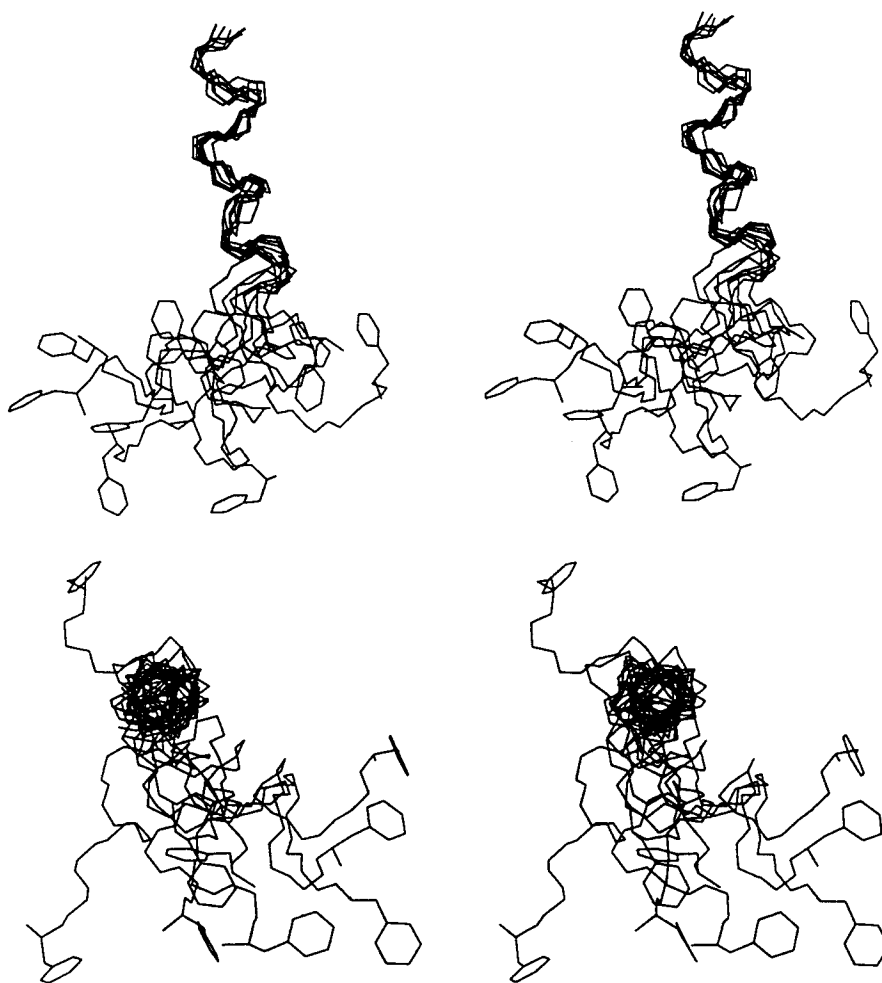


FIGURE 4 (A) Stereo views showing the superimposition of the backbone atoms (N, C α , C') over residues Aib-1 to Aib-10 of 9 of the 24 DG/SA structures. The side-chain atoms of phenylalaninol-20 are also drawn to indicate the C-terminus. The average backbone rmsd is 1.1 ± 0.4 Å over the region 1–10. The 9 DG/SA molecules superimpose on the three crystal structures with an average backbone rmsd of 0.94 ± 0.39 Å. (B) A stereoview of the same molecules as in panel A but looking down the N-terminal helix.

connected by a disordered region around Gly-11/Leu-12, though the helices are more disordered than in the family described above. A second family of DG/SA structures was generated by including in the DG/SA algorithm hydrogen-bonding constraints deduced from the temperature dependence of the NH resonances (Figure 3A). Structures were generated with four 3_{10} interactions in the N-terminus and either five α interactions or five 3_{10} interactions in the C-terminus. The resultant structures resemble the structures described above, except that the termini of the molecule are better constrained. Low energy structures were produced when the C-terminus was constrained to be either α - or 3_{10} -helical.

Thus the NOE and coupling constant constraints are compatible with both types of conformation at the C-terminus.²⁵

DISCUSSION

Dynamics

Recently, progress has been made in defining the structures in solution of short, highly helical, alanine-based peptides.²⁹ The placement of a single glycine^{30,31} or proline³⁰ near the center of these peptides dramatically reduces their helicity. Alamethicin is a 20 amino acid peptide with a glycine

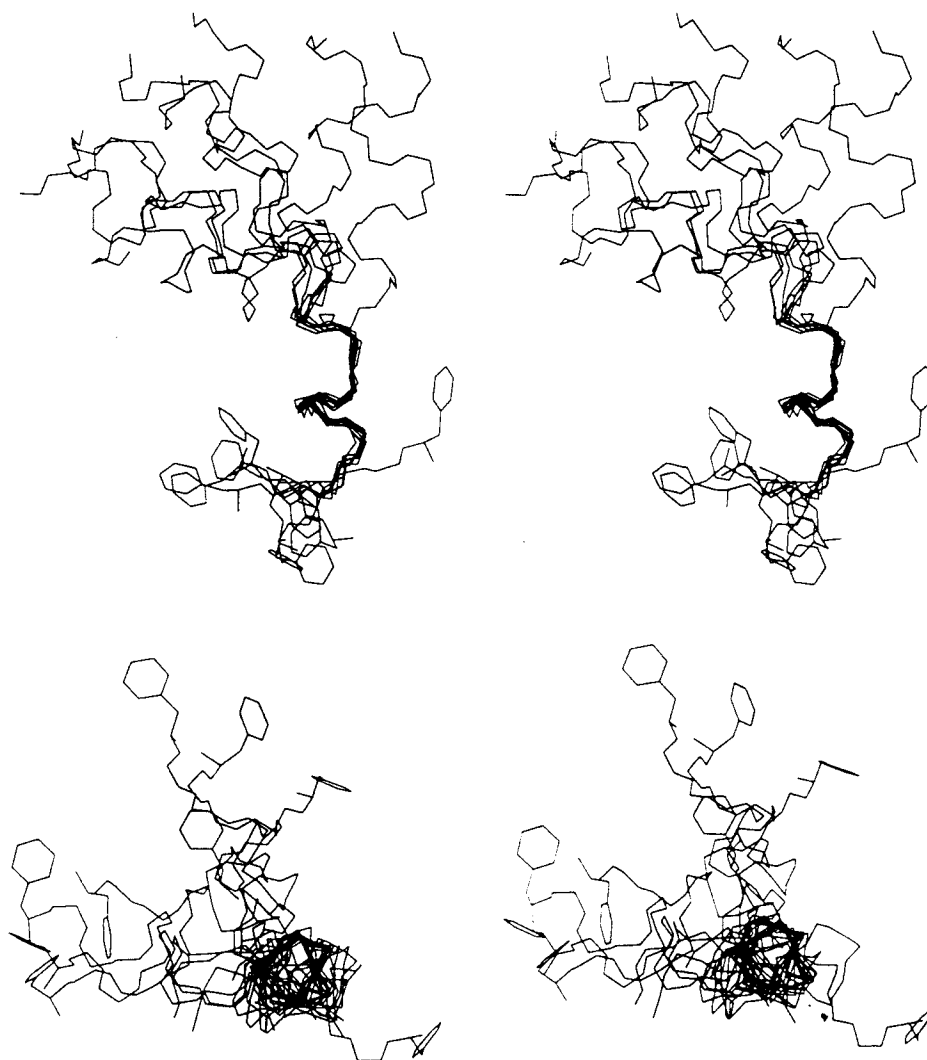


FIGURE 5 (A) Stereo views showing the superimposition of the backbone atoms (N, C α , C') over residues Leu-12 to Gln-17 of 9 of the 24 DG/SA structures. The side-chain atoms of phenylalanine-20 are also drawn to indicate the C-terminus. The average backbone rmsd is 0.52 ± 0.21 Å over the region 12–17. The family of 9 DG/SA molecules superimpose on the three crystal structures with an average backbone rmsd of 0.43 ± 0.11 Å. (B) A stereoview of the same molecules as in panel A but looking up the C-terminal helix.

and a proline near the middle of the peptide, yet it exhibits many characteristics of a stable helix in solution including a strongly helical CD spectrum. However, nmr-based structure determination is hampered by the preponderance of Aib residues, which lack α H resonances, and the two proline residues, which lack NH resonances. This reduces, for example, the number of measurable $^3J_{\alpha,N}$ to 6 and the number of $\alpha,N(i,i+3)$ NOEs to 9, of which 8 are observed. Because the 16 Aib methyl protons have very similar chemical shifts, resolution of NOEs to these resonances is difficult and further

reduces the number of measurable distance restraints.

The lack of observable nmr constraints leads to some of the conformational heterogeneity observed in the DG/SA structures (Figures 4–7). However, the heterogeneity in the conformations at Gly-11/Leu-12 most likely reflects conformational freedom in solution. This conclusion is supported by the random coil chemical shifts of these residues (Figure 2), the temperature dependence of their amides (Figure 3), and the $^3J_{\alpha,N}$ of Leu-12 (7.9). Dynamics at Gly-11/Leu-12 was first

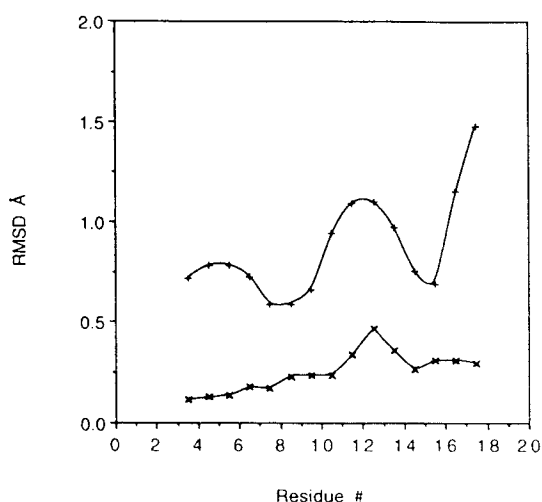


FIGURE 6 Averages of pairwise rmsds for backbone heavy atoms (N, C α , C') were calculated over 6 amino acid segments and plotted in the middle of each segment. The (+) indicates 24 alamethicin DG/SA structures; (x) indicates 3 alamethicin crystal structures.⁷

predicted³² using molecular dynamics calculations. We (unpublished observations) and others³³ have observed a similar effect in the peptide dissolved in detergent. A flexible hinge region could be important in the opening and closing of pores in response to applied voltage. On the other hand, a popular model of channel gating involves a rigid helix macrodipole responding to applied voltage.¹⁵ The observed flexibility of the peptide in its center casts this mechanism in some doubt.³³

There is also evidence that the two helical regions identified in Figures 4 and 5 are dynamic in solution. Only 1 $\alpha, N(i, i + 4)$ NOE and 2 of the possible 6 $\alpha, \beta(i, i + 3)$ NOEs are measured, suggesting that the helices are flexible. An alternative explanation is that the molecule, or parts of it, adopts a stable 3_{10} conformation that would reduce the intensity of the $(i, i + 3)$ and $(i, i + 4)$ NOEs.²⁵ The temperature dependence of the amide chemical shifts of Aib-3 and Ala-4 (Figure 3) are evidence that these residues are involved in 3_{10} hydrogen bonds at the very end of the molecule. The $\alpha, N(i, i + 4)$ NOE suggests that the molecule switches to an α -helical conformation between residues 4 and 10, or that in solution the molecule exists in a state of flux between the two states.³⁴ It has been speculated¹⁶ that an $\alpha \rightarrow 3_{10}$ transition may be important in the voltage-regulated gating of peptide-based ion channels. Mixed $3_{10}/\alpha$ -helical conformations of peptides containing multiple Aibs are not uncommon,³⁵⁻³⁷ and acetylated alanine-

based peptides have been observed to form 3_{10} conformations at their ends and α -helical conformations in the middle of the peptides.³⁸

The observation of several 3_{10} interactions in the C-termini of the alamethicin crystal structures¹² could not be confirmed in the DG/SA calculations. This is not surprising as coupling constants and NOE patterns are very similar for the two conformations.²⁵ However, the conformations of the

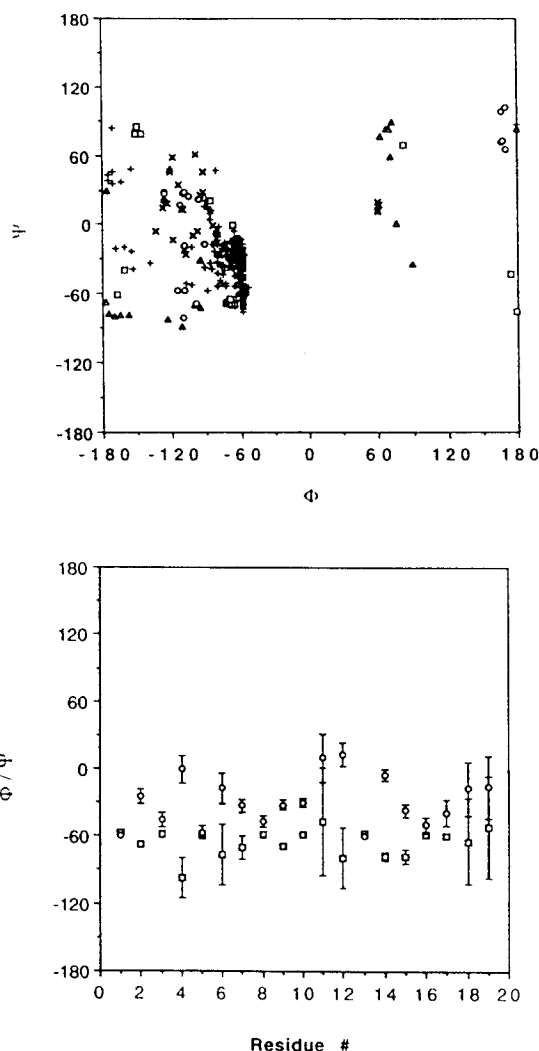


FIGURE 7 (A) Ramachandran plot of the 24 DG/SA structures. (○) Gly-11, (×) Leu-12, (□) Gln-18, (Δ) Gln-19, and (+) all other amino acids. (B) Average backbone dihedral Φ and Ψ angles and their confidence intervals as a function of residue number. Confidence intervals were calculated from the standard deviations (S) of the data using the formula $x \pm t_{S^2} S/\sqrt{n}$ where x is the mean, n is the number of measurements, and t_{S^2} is the deviation of the estimated mean from the population mean at a 95% confidence level.⁴³

peptide shown in Figures 4 and 5, and the analysis shown in Figures 6 and 7, suggest that the peptide is less well constrained in the C-terminus than in the N-terminus. The weak dependence on temperature of the amide chemical shifts (Figure 3) suggests that this is due at least in part to a lack of NOE data at the end of the linear conformation. It suggests that the C-terminal helix may be as well defined as the N-terminus.

Chemical Shift

Jung et al.⁴ have shown that Aib methyl carbon chemical shifts are sensitive to peptide secondary structure and dynamics. The *pro-R* and *pro-S* ¹³C methyls of Aib are magnetically equivalent in the blocked amino acid as the molecules are achiral and apparently conformationally flexible.³⁹ In chiral di- and tripeptides containing Aib the *pro-R* and *pro-S* carbons are shifted apart by up to 2 ppm.³⁹ In these chiral compounds the β -carbons are diastereotopic and it is not possible to distinguish, from the chemical shifts alone, if the molecules are rigid or flexible in solution.⁴⁰ In larger peptides containing 3–10 residues, the Aib methyls are shifted apart by 2–4 ppm. Figure 1 indicates that in alamethicin the chemical shift differences among the *pro-R* and *pro-S* diastereotopomers are small. For example, the *pro-S* ¹³C-methyl of Aib-1 is shifted about 0.5 ppm downfield of the ¹³C-methyl of Aib-5. The magnitude of this chemical shift difference is likely due to differences in local sequence and chirality near each of the Aib residues. Aib-1 contains no chiral substituents on its N-terminus and Aib-10 is bonded to achiral Gly-11. In addition to these small differences due to local sequence, there is a large 4 ± 0.5 ppm chemical shift difference between the *pro-R* and *pro-S* methyl carbons of all the Aib residues. That the magnitude of this difference is nearly identical for all of the residues suggests that the effect is due to a local interaction common to all the Aibs. As suggested,⁴ in a right-handed helical conformation the *pro-R* methyl is proximate to the Aib carbonyl oxygen, causing it to be deshielded relative to the *pro-S* carbon. These results suggest that all the Aib residues in alamethicin are rigidly constrained to the right-handed helical conformation in methanol and that any conformational flexibility is a consequence of dynamics at non-Aib residues.

The Aib NH resonances are also interesting as they span a wide range of chemical shifts. This suggests that the molecule, or at least parts of it, are stably folded in methanol. The main contribution

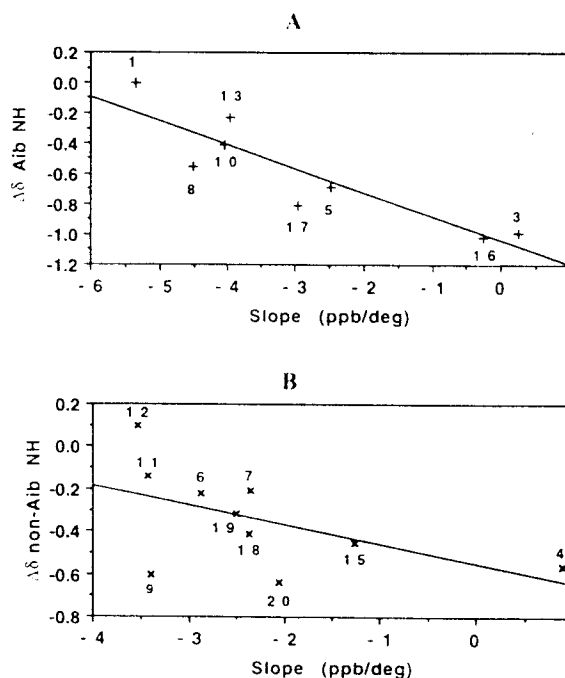


FIGURE 8 (A) Correlation between the Aib amide proton chemical shift differences from Aib-1 and their temperature dependencies. (B) Correlation between the non-Aib amide proton chemical shift differences from the random coil values and their temperature dependencies. The data for this plot can be found in Figures 2C and 3.

to NH chemical shift differences in proteins is the strength of the NH hydrogen bonding interaction.²³ Thus, the Aib NHs likely participate in a wide range of hydrogen bond strengths, which suggests a range of conformational flexibility throughout the length of the peptide. This conclusion is supported by measurements of the temperature sensitivity of the NH chemical shifts (Figure 3A), which indicate that the most shielded (helical) Aib NH resonances^{3,16} (Figures 3A and 8A) are also the least sensitive to temperature. Conversely, the most deshielded (random) NHs have the highest temperature sensitivity^{1,13} (Figures 3A and 8A), indicating no hydrogen bond at the very N-terminus and a weakened secondary structure in the middle of the molecule near Gly-11.

The correlation between the temperature dependence of the NH chemical shift and the chemical shift relative to the random coil value holds for at least 6 of the non-Aib residues as well (Figure 8B). The deviations from a linear correlation are interesting and may be attributable to a helix macrodipole. It has been postulated²³ that at the N-terminus of an α -helix partial positive charge,

normally localized on the four terminal amide hydrogens, may deshield the amides, whereas the partial negative charge at the C-terminus could shield the amides. The calculated²³ average chemical shift for the three N-terminal amide protons (including the N-1 position) in 67 helices from randomly selected proteins was 8.58 ± 0.46 ppm. The average C-terminal chemical shift was 7.80 ± 0.36 ppm. The downfield shift of Aib-1 (8.61 ppm) (Figure 8A) and the upfield shifts of Pho-20 (7.29 ppm) (Figure 8B) might be attributable to such a helix dipole phenomenon. However, note as well that the NHs of Leu-12 and perhaps Aib-13 are shifted downfield from their positions predicted from the temperature dependence of their chemical shifts, and that the NHs of Aib-8, Val-9, and Aib-17 are shifted upfield. One explanation is that the N-terminal helix spans residues 1–9 and the C-terminal helix spans residues 12–17 or 20. The response of an alamethicin helix dipole to an applied voltage is an important element in a model for channel gating.⁴¹ The present results suggest that the macrodipole may form in response to an applied voltage from two preexisting helical dipoles in the N- and C-termini of the protein.

Recently, nmr-constrained conformations of alamethicin dissolved in a detergent were published.³³ In general, there is good agreement between the results of the two studies, although the 3_{10} interaction at the N-terminus was not observed in detergent. On the basis of theoretical^{1–3,15,16} and experimental evidence (see above), we constrained all the Aib residues to be right-handed helical (α or 3_{10}) and therefore do not observe any conformational heterogeneity at Aib-10, as was reported for the molecule in detergent.³³ The suggestion has been made that the lack of a hydrogen-bonding partner at Pro-14 may reduce constraints on Aib-10, making it more flexible. Proline residues are well known for putting bends in helices⁴²; however, in the crystal, the Aib-10 carbonyl in molecule III is hydrogen bonded in an ($i, i + 3$) interaction with the NH of Aib-13.¹² Examination of the present chemical shift data, and the temperature dependence of the amides, suggests that conformational flexibility as measured by hydrogen-bond strength is greater at Aib-13 than at Aib-10. We conclude that the hinge in alamethicin is restricted to Gly-11/Leu-12, that helical hydrogen bonds are weakened in this region, but that the Aib residues experience relatively little intrinsic conformational flexibility.

We thank Mr. Kirk Marat and Mr. Terry Wolowicz for

maintaining the nmr spectrometers in excellent working order. This research was supported by the Natural Sciences and Engineering Research Council of Canada.

REFERENCES

- Burgess, A. W. & Leach, S. J. (1973) *Biopolymers* **12**, 2599–2605.
- Paterson, Y., Rumsey, S. M., Benedetti, E., Nemethy, G. & Scheraga, H. A. (1981) *J. Am. Chem. Soc.* **103**, 2947–2955.
- Toniolo, C., Crisma, M., Formaggio, F., Valle, G., Cavicchioni, G., Precigoux, G., Aubry, A. & Kamphuis, J. (1993) *Biopolymers* **33**, 1061–1072.
- Jung, G., Bruckner, H., Bosch, R., Winter, W., Schaal, H. & Strahle, J. (1983) *Liebigs Ann. Chem.* 1096–1106.
- Karle, I. & Balaran, P. (1990) *Biochemistry* **29**, 6747–6761.
- Marshall, G. R., Hodgkin, E. E., Langs, D. A., Smith, G. D., Zabrocki, J. & Leplawy, M. T. (1990) *Proc. Natl. Acad. Sci. US* **187**, 487–491.
- Prasad, B. V. V. & Balaran, P. (1984) *CRC Crit. Rev. Biochem.* **16**, 307–348.
- Basu, G. & Kuki, A. (1993) *Biopolymers* **33**, 995–1000.
- Basu, G., Kubasik, M., Demetrios, A., Secor, B. & Kuki, A. (1990) *J. Am. Chem. Soc.* **112**, 9410–9411.
- DeGrado, W. F. & Lear, J. D. (1990) *Biopolymers* **29**, 205–213.
- Meyer, C. E. & Reusser, F. (1967) *Experientia* **23**, 85–86.
- Fox, R. O. & Richards, F. M. (1982) *Nature* **300**, 325–330.
- Sansom, M. S. P. (1993) *Eur. Biophys. J.* **22**, 105–124.
- Woolley, G. A. & Wallace, B. A. (1992) *J. Membrane Biol.* **129**, 109–136.
- Basu, G., Bagchi, K. & Kuki, A. (1991) *Biopolymers* **31**, 1763–1774.
- Huston, S. E. & Marshall, G. R. (1994) *Biopolymers* **34**, 75–90.
- Yee, A. A. & O'Neil, J. D. J. (1992) *Biochemistry* **31**, 3135–3143.
- Bodenhausen, G. & Ruben, O. J. (1980) *Chem. Phys. Lett.* **69**, 185–189.
- Shaka, A. J., Barker, P. B. & Freeman, R. (1985) *J. Magn. Reson.* **64**, 547.
- Redfield, A. G. & Kunz, S. D. (1975) *J. Mag. Reson.* **63**, 250–254.
- Eposito, G., Carver, J. A., Boyd, J. & Campbell, I. D. (1987) *Biochemistry* **26**, 1043–1050.
- Kelsh, L. P., Ellena, J. F. & Cafiso, D. S. (1992) *Biochemistry* **31**, 5136–5144.
- Wishart, D. S., Sykes, B. D. & Richards, F. M. (1991) *J. Mol. Biol.* **222**, 311–333.

24. Spera, S. & Bax, A. (1991) *J. Am. Chem. Soc.* **113**, 5490-5492.
25. Wüthrich, K. (1986) *NMR of Proteins and Nucleic Acids*. John Wiley, New York.
26. Clore, G. M., Gronenborn, A. M., Nigles, M. & Ryan, C. A. (1987) *Biochemistry* **26**, 8012-8023.
27. Wagner, G., Braun, W., Havel, T. S., Schaumann, T., Go, N. & Wüthrich, K. (1987) *J. Mol. Biol.* **196**, 611-639.
28. Blake, P. R., Park, J.-B., Zhou, Z. H., Hare, D. R., Adams, M. W. W. & Summers, M. F. (1992) *Protein Sci.* **1**, 1508-1521.
29. Scholtz, J. M. & Baldwin, R. L. (1992) *Ann. Rev. Biophys. Biomol. Struct.* **21**, 95-118.
30. Merutka, G., Lipton, W., Shalango, W., Park, S.-H. & Stellwagen, E. (1990) *Biochemistry* **29**, 7511-7515.
31. Chakrabarty, A., Schellman, J. A., & Baldwin, R. L. (1991) *Nature* **351**, 586-588.
32. Fraternali, F. (1990) *Biopolymers* **30**, 1083-1099.
33. Franklin, J. C., Ellena, J. F., Jayasinghe, S., Kelsh, L. P. & Cafiso, D. S. (1994) *Biochemistry* **33**, 4036-4045.
34. Williamson, M. P. & Waltho, J. P. (1992) *Chem. Soc. Rev.* **21**, 227-236.
35. Karle, I. L., Flippen-Anderson, J., Sukumar, M. & Balaram, P. (1987) *Proc. Natl. Acad. Sci. USA* **84**, 5087-5091.
36. Pavone, V., Benedetti, E., Diblasio, B., Pedone, C., Santini, A., Bavaso, A., Toniolo, C., Crisma, M. & Sartore, L. (1990) *J. Biomol. Struct. Dynam.* **7**, 1321-1331.
37. Basu, G. & Kuki, A. (1992) *Biopolymers* **32**, 61-71.
38. Fiori, W. R., Siobhan, M. M. & Millhauser, G. L. (1993) *Biochemistry* **32**, 11957-11962.
39. Leibfritz, D., Haupt, E., Dubischar, N., Lachmann, H., Oekonomopulos, R. & Jung, G. (1982) *Tetrahedron* **38**, 2165-2181.
40. Jennings, W. B. (1975) *Chem. Rev.* **75**, 307-322.
41. Boheim, G., Hanke, W. & Jung, G. (1983) *Biophys. Struct. Mech.* **9**, 181-191.
42. Barlow, D. J. & Thornton, J. M. (1988) *J. Mol. Biol.* **201**, 601-619.
43. Snedecor, G. W. & Cochran, W. G. (1980) *Statistical Methods*, 7th ed., The Iowa State University Press, Ames, IA, USA.